Mild oxidation of alkenes catalyzed by Fe_3O_4/SiO_2 nanoparticles

**Mohammad Ali Nasseri · Ali Allahresani ·
Heidar Raissi**

Abstract   In this work, Fe_3O_4/SiO_2 nanoparticles were synthesized according to the literature and characterized by transmission electron microscopy, powder X-ray diffraction, Fourier transform infrared spectroscopy, thermogravimetric analysis and vibrating sample magnetometer. The catalytic properties of the Fe_3O_4/SiO_2 catalyst have been tested in the epoxidation of different cyclic and acyclic alkenes with m-chloroperbenzoic acid (oxidizing agent). Under optimized conditions, all reactions afforded the desired products in good to excellent yields. Furthermore, the effect of different additives such as pyridine N-oxide and N-methylmorpholine-N-oxide was tested on the conversion of alkenes, but in all cases additives did not improve epoxidation yields. As a result, the Fe_3O_4/SiO_2 showed good activity and super stability in the epoxidation of various olefins. Moreover, this catalyst can be recovered by using a magnetic field and recycled for several times without a significant loss in the catalytic activity.

Keywords Fe_3O_4/SiO_2 · Alkenes · Epoxidation · Magnetic nanoparticles

Introduction

Selective epoxidation of alkenes into high value chemicals (epoxides) which are widely used in the fine chemical industry is of great attention in chemical and pharmaceutical industries [1]. Some transition metal oxides such as NiO, CoO, MoO_3, CuO, TiO_2–SiO_2, Au/SiO_2, $CuOx/SiO_2$ and tungstate(VI) or molybdate(VI) have been reported for the epoxidation of alkenes with organic hydroperoxides [2–8]. However, in most cases, either alkene conversion or alkene oxide selectivity/ yield was poor and many of these transition metal catalysts are expensive and highly

M. A. Nasseri (✉) · A. Allahresani · H. Raissi
Department of Chemistry, Faculty of Sciences, University of Birjand, Birjand, Iran
e-mail: manaseri@birjand.ac.ir

dangerous for the environment as well. From an economic point of view, the separation of ultrascaled and nanosized catalysts from the reaction system via routine methods such as free sedimentation, centrifuging and filtration is difficult, time-consuming and costly. Magnetic nanoparticles (NPs) which are economic friendly can be easily separated by applying a simple external magnet without any significant loss of activity put forward a solution to this problem. In addition, good selectivity and great stability are some especial advantageous of magnetic NPs [9–11]. Magnetic NPs have been reported to catalyze a wide range of reactions including, C–C, C–S, C–N bond formation, asymmetric synthesis and oxidations reactions [12–15]. Usually, silica was utilized to coat the Fe_3O_4 particles forming Fe_3O_4/SiO_2 core–shell structure. This layer not only protects Fe_3O_4 from oxidizing or dissolving in the acidic reaction media, but also stabilizes NPs by preventing aggregation of the Fe_3O_4 particles [16]. The silica shell can also provide numerous surface Si–OH groups for further modification [17, 18].

This article presents the epoxidation of cyclic and acyclic alkenes with m-chloroperbenzoic acid (m-CPBA) in the presence of catalytic amount of Fe_3O_4/SiO_2 NPs in dichloromethane as solvent. By using this catalyst, the corresponding products were obtained in excellent yields after 4 h and magnetic NPs, which are recovered from the reaction mixture by using external magnetic field simplified the isolation of products (Fig. 1).

Experimental

General

Tetraethoxysilane (TEOS), $FeCl_3·6H_2O$, $FeCl_2·4H_2O$, styrene, 4-chlorostyrene, cyclohexene, α-methyl styrene, indene, cis- and trans-stilbene, cyclohexene, cyclooctene, 1-octene, m-CPBA, pyridine N-oxide (PNO), pyridine (Py), N-methylmorpholine-N-oxide (NMNO), 1-methylimidazole (MI), imidazole, dichloromethane (DCM), ethyl acetate (EtOAC), ethanol (EtOH), CH_3CN, $CHCl_3$, THF, $NaIO_4$, NH_4OAC, t-BOOH, $PhI(OAC)_2$, H_2O_2 (30 %) and Oxone were purchased from Merck and used without purification. Graphite powder was obtained from Aldrich. The resulting Fe_3O_4/SiO_2 was characterized by IR, TEM, TGA, VSM and X-ray diffraction (XRD) patterns. The IR experiments were carried out on a Perkin-Elmer 783 Infrared spectrophotometer in a KBr pellet, scanning from 4,000 to 600 cm^{-1} at room temperature. The XRD measurements were carried out by using a Bruker D_8-advance X-ray diffractometer with Cu $K_α$ radiation (k = 1.5406 Å). The TEM images measurements were obtained using Philips CM10 instrument. Magnetization measurements were carried out at 300 K on a vibrating sample magnetometer (VSM Leak shore 7200). The TGA analysis was performed by heating the samples in an argon flow at a rate of 100 mL min^{-1} using a Perkin–Elmer Diamond TG/DTA thermal analyzer with a heating rate of 10 °C min^{-1}. The conversion of products was determined by GC-17A Shimadzu with capillary column (Shimadzu, CBP5, 30 m × 25 mm × 0.25 μm).

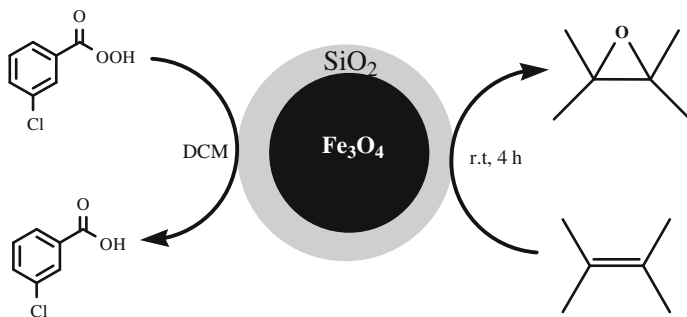**Fig. 1** Epoxidation of alkenes with m-CPBA catalyzed by Fe_3O_4/SiO_2 in dichloromethane solvent. Reaction conditions: alkene (1 mmol), m-CPBA (2 mmol), catalyst (0.06 g), DCM (3 mL) 4 h at room temperature

General procedure for the synthesis of Fe_3O_4/SiO_2 core–shell

Black magnetic Fe_3O_4 NPs were prepared as described in the literature [19]. The core–shell Fe_3O_4/SiO_2 NPs were prepared by a modified Stober method [20]. Briefly, Fe_3O_4 (0.50 g, 2.1 mmol) was dispersed in the mixture of ethanol/deionized water (50:5 mL). Then, TEOS (0.20 mL) was slowly added to the mixture followed by addition of 5 mL of NaOH (10 wt%). This solution was stirred mechanically for 20 h at room temperature. Then the product, Fe_3O_4/SiO_2, was separated by an external magnet, washed with deionized water and ethanol three times and dried at 80 °C for 10 h.

General procedure for the epoxidation of olefins

In a typical procedure, the catalyst (0.06 g) was dispersed in 3 mL of dichloromethane for 10 min. Then the substrate (1 mmol) and m-CPBA (2 mmol) were added to the mixture at room temperature. The mixture was stirred at room temperature for appropriate times. The progress of the reaction was monitored by TLC. After the completion of the reaction, the catalyst was separated by external magnet. The solution was washed with 1 M NaOH (8 mL) and brine (8 mL) and dried over $MgSO_4$. Then, the solution was concentrated by rotary evaporator to 1 mL. Finally, the conversion of the products was determined by GC. The catalyst was washed twice with ethanol and reused.

Results and discussion

Characterizations of catalyst

The Fe_3O_4 NPs (A) were simply synthesized by using of $FeCl_3 \cdot 6H_2O$ and $FeCl_2 \cdot 4H_2O$ in deionized water under nitrogen atmosphere. Then, Fe_3O_4/SiO_2 NPs

were obtained by treating the Fe_3O_4 NPs with TEOS (Fig. 2). The magnetic properties of the Fe_3O_4 and Fe_3O_4/SiO_2 NPs (B) were studied by a VSM at 300 k. As shown in Fig. 3, both NPs have super paramagnetism at room temperature. Also, no hysteresis phenomenon was observed in Fig. 3 and the saturation magnetization values for Fe_3O_4 and Fe_3O_4/SiO_2 NPs were 70.495 and 38.30 emu/g, respectively. However, despite the considerable decrease of the magnetization of Fe_3O_4/SiO_2 NPs compared to Fe_3O_4, Fe_3O_4/SiO_2 NPs can still be separated from the solution by using an external magnetic field on the sidewall of the reactor. Fig. 4a shows the IR spectrum of Fe_3O_4 with important vibration bands in 560–590 and 3,400 cm^{-1}, which are due to Fe–O and OH, respectively. According to the IR spectrum of Fe_3O_4/SiO_2 in Fig. 4b, there are several important vibration bands in 560–590, 954, and 3,400 cm^{-1}, which are due to Fe–O, Si–OH, and OH. The vibration bands in 755 and 1,100 cm^{-1} are due to Si–O–Si. These vibration bands (755, 954 and 1,100 cm^{-1}) confirmed coating of the silica shell on the surface of the Fe_3O_4 NPs.

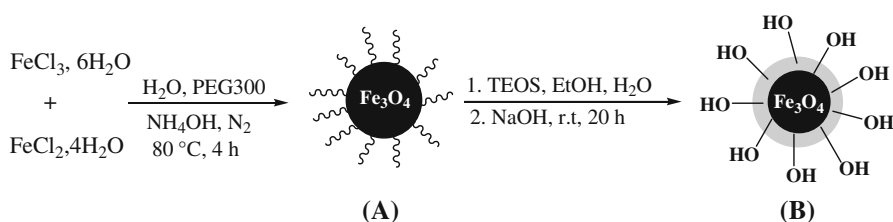**Fig. 2** Schematic illustration for synthesis of Fe_3O_4 (**a**) and Fe_3O_4/SiO_2 (**b**). Reaction conditions: $FeCl_3·6H_2O$ (4.8 mmol g), $FeCl_2·4H_2O$ (4.5 mmol), water (30 mL), NH_4OH (pH 10), PEG (1 g), N_2, 80 °C, 1 h (**a**) and Fe_3O_4 (2.1 mmol), ethanol/deionized water (50:5 mL), TEOS (0.20 mL), of NaOH (10 wt%, 5 mL) 20 h at room temperature (**b**)
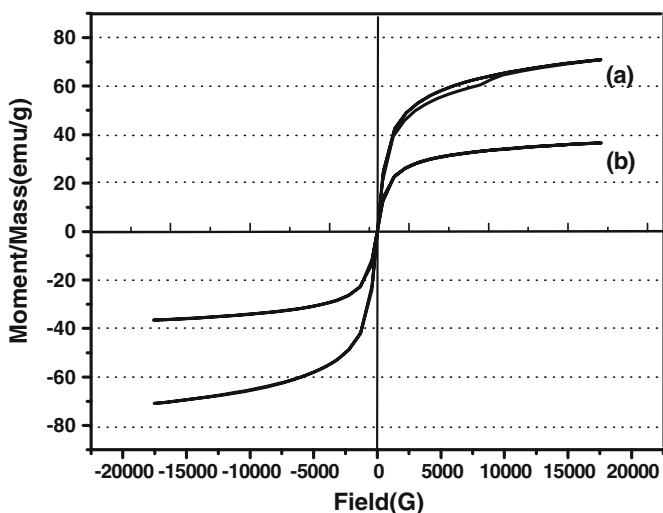

Fig. 3 Magnetization curves of **a** Fe_3O_4 NPs. **b** Fe_3O_4/SiO_2 NPs at 300 K. The Fe_3O_4/SiO_2 NPs can be separated easily with external magnet
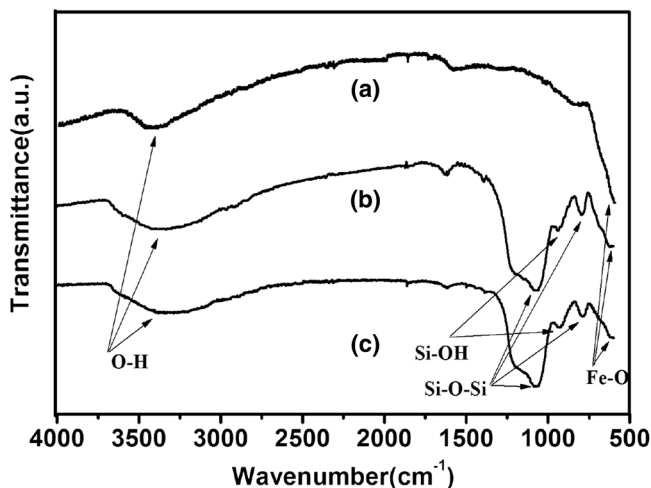
Fig. 4 FT-IR spectra of **a** fresh Fe_3O_4 **b** the fresh Fe_3O_4/SiO_2 catalyst and **c** the Fe_3O_4/SiO_2 catalyst of cycle 5
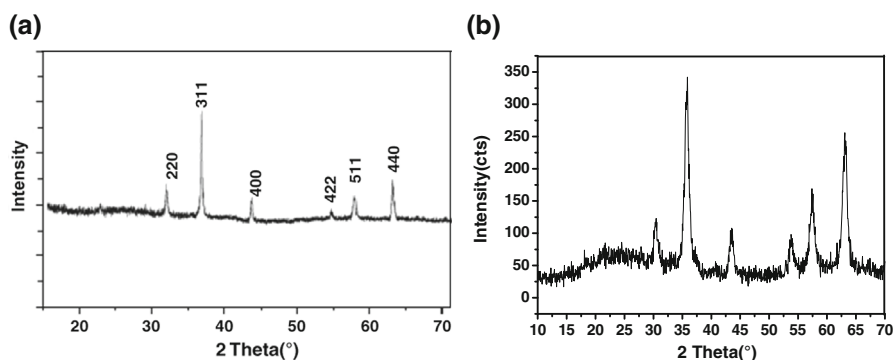

Fig. 5 XRD pattern of **a** fresh Fe_3O_4 **b** the fresh Fe_3O_4/SiO_2 catalyst which are in good agreement with the literature value (JCPDS Card No. 19-0629)

The XRD pattern of Fe_3O_4 and Fe_3O_4/SiO_2 NPs were determined by powder XRD. As shown in Fig. 5a, the pattern of Fe_3O_4 indicates a crystallized structure at 2θ: 30.2°, 35.4°, 43.3°, 53.6°, 57.5° and 63.1° which are assigned to the (220), (311), (400), (422), (511) and (440) crystallographic faces of magnetite, which is in good agreement with the literature value (JCPDS Card No. 19-0629). The XRD pattern of Fe_3O_4/SiO_2 presents almost the same feature as shown in Fig. 5b. The broad peak at $2\theta = 15$–27°, which depends on amorphous silica. The average diameter of Fe_3O_4 was about 11 nm, while the diameter of Fe_3O_4/SiO_2 was about 14 nm, which is due to the agglomeration of Fe_3O_4 inside nanospheres and surface growth of silica on the shell. The SEM image of Fe_3O_4 shows the
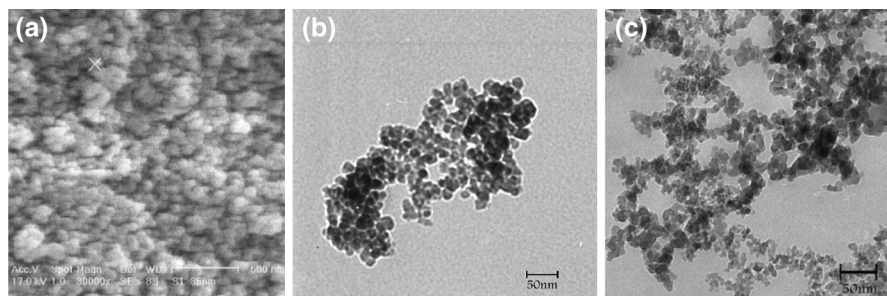
Fig. 6 SEM images of **a** Fe$_3$O$_4$, **b** TEM micrographs of Fe$_3$O$_4$ and **c** TEM images of Fe$_3$O$_4$/SiO$_2$
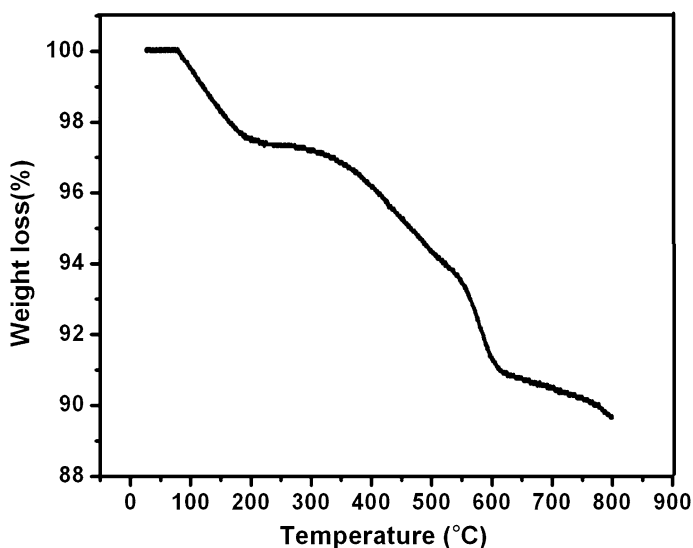
Fig. 7 Thermogravimetric weight loss pattern of Fe$_3$O$_4$/SiO$_2$NPs with temperature raised of 10 °C/min and initial sample weigh of 4.9 mg

morphology and average product size of Fe$_3$O$_4$ NPs (Fig. 6a). The TEM images of Fe$_3$O$_4$ and Fe$_3$O$_4$/SiO$_2$ NPs are shown in Fig. 6b, c. The results showed the average product size of Fe$_3$O$_4$ and Fe$_3$O$_4$/SiO$_2$ NPs 10 and 13 nm similar to the results of XRD patterns. The TEM images of Fe$_3$O$_4$/SiO$_2$ NPs indicate the successful coating of magnetic Fe$_3$O$_4$ NPs (Fig. 6c). The TGA curve of Fe$_3$O$_4$/SiO$_2$ shows a weight loss over the range of 90–160 °C of about 3 %. These losses can be attributed to the loss of adsorbed water and dehydroxylation of internal OH groups. The second weight loss step is over the range 250–590 °C, which can be ascribed to even further decomposition of the materials. The total weight losses are approximately 10 % (Fig. 7).

Catalytic activity

In this study, Fe_3O_4/SiO_2 NPs were tested to catalyze the selective oxidation of alkenes using m-CPBA as an oxidant. Styrene was selected as model substrate and treated with Fe_3O_4/SiO_2 NPs in the presence of m-CPBA as the oxygen donor at room temperature under different conditions. This reaction was best carried out using 2 equiv. of m-CPBA for 4 h at room temperature in dichloromethane. The catalytic activity of the Fe_3O_4 NPs was also investigated in the epoxidation of styrene, and low yield (45 %) was observed. Blank experiments showed that Fe_3O_4 and Fe_3O_4/SiO_2 NPs alone are inactive towards the styrene epoxidation. To optimize the amount of catalyst, the reaction was carried out in the presence of different amount of Fe_3O_4/SiO_2 NPs (0.01–0.08 g) at room temperature. It was found that 0.06 g of Fe_3O_4/SiO_2 was sufficient enough to afford styrene oxide with 97 % isolated yield (Table 1, entry 6).

To explore the effect of solvent on the reaction, the same reactions were performed in different solvents. Despite the moderate yields in some solvent such as EtOAC and CH_3CN (Table 2, entries 1, 2), the best conversion was observed when the reaction was performed in DCM (Table 1, entry 7, 97 %).

Table 1 Optimization of the catalyst amount of Fe_3O_4/SiO_2 NPs

Entry	Catalyst amount (g)	Time (h)	Yield[a] (%)
1	0.01	4	15
2	0.02	4	25
3	0.03	4	40
4	0.04	4	58
5	0.05	4	78
6	0.06	4	97
7	0.07	4	98
8	No catalyst	4	8

Reaction conditions: styrene (1 mmol), m-CPBA (2 mmol), DCM (3 mL) at room temperature

[a] Determined by GC with a CBP5 column (Shimadzu 30 m × 0.32 mm × 0.25 mm)

Table 2 The effect of solvent on the conversion of styrene to the corresponding styrene oxide

Entry	Solvent	Time (h)	Yield[a] (%)
1	EtOAC	4	75
2	CH_3CN	4	60
3	H_2O	4	15
4	$EtOH:H_2O$	4	40
5	$CHCl_3$	4	50
6	THF	4	35
7	CH_2Cl_2	4	97

Reaction conditions: styrene (1 mmol), m-CPBA (2 mmol) and catalyst (0.06 g) at room temperature

[a] Yields refer to GC yield

The effect of different oxidants and additives in the epoxidation of styrene

The effect of various oxidants such as $NaIO_4$, m-CPBA, UHP, H_2O_2, Oxone, PhIO, $PhI(OAC)_2$ and tert-BuOOH was investigated in the epoxidation of styrene. The results showed that m-CPBA is the best oxygen source because this oxidant can give better yield (Table 3, entry 1) while other oxidants such as UHP, H_2O_2, PhIO, $PhI(OAC)_2$ gave low yields (Table 3, entries 5–8). In addition, different equivalents of the oxidant were tested, and the best catalytic activity was obtained with 2 equivalents of the oxidant which provide moderate source of oxygen for the catalytic reaction. Also, dichloromethane was chosen as the best reaction medium. Consequently, the optimum molar ratio of olefin to oxidant is 1:2.

The effect of various additives such as NMNO, PNO, NH_4OAC, MI, Py and imidazole was investigated in the epoxidation of styrene in the DCM/m-CPBA system. Generally, additives such as NMNO and imidazole in the Mn(III) salen reaction mixture facilitate faster reaction rates and higher epoxide yields. However, in this test, the catalytic activity did not increase in the presence of PNO and other additives.

The reactions were also carried out in 0, 40 and 60 °C. The yield was lower at 0 °C than at room temperature, but both of them showed good selectivity. When the reactions were carried out in 40 and 60 °C, the reaction rates increased but the selectivity of epoxides decreased. So, considering the economic point of view and selectivity, room temperature was chosen as the best condition for this reaction. Therefore, we employed the optimized conditions (0.06 g nanocatalyst, 2 mmol m-CPBA and DCM at room temperature) for the conversion of several alkenes into the corresponding products. Table 4 lists a group of alkenes that were investigated by magnetic NPs catalysts. The catalyst showed excellent activity toward alkenes oxidation with an average isolation yield of 95 %.

The efficiency of Fe_3O_4/SiO_2 is compared in Table 5 with the earlier reported ones for their styrene epoxidation activity, expressed in terms of selectivity and yields for the styrene oxide formation. Usually, transition metals are not very highly efficient catalysts for alkene epoxidation (Table 5, entries 1–12). The comparisons
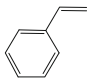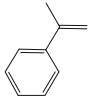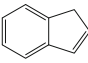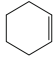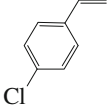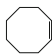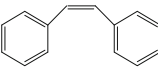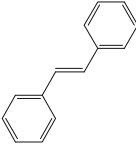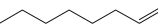
Table 3 The effect of different oxidants on the conversion of styrene to the corresponding Styrene oxide

Entry	Oxidant	Time (h)	Yield[a] (%)
1	m-CPBA	4	97
2	Oxone	4	65
3	tert-BuOOH	4	70
4	$NaIO_4$	4	50
5	UHP	4	35
6	PhIO	4	25
7	H_2O_2	4	20
8	$PhI(OAC)_2$	4	15

Reaction conditions: styrene (1 mmol), solvent (3 mL) and catalyst (0.06 g) at room temperature

[a] Yields refer to GC yield

Table 4 Epoxidation of different alkenes catalyzed by Fe₃O₄/SiO₂ nanoparticles

Entry	Alkene	Time (h)	Selectivity %	T ($^{\circ}$C)	Yield[a] (%)
1		4	99	25	97
2		4	99	25	97
3		4	98	25	97
4		4	99	25	95
5	Cl	4	99	25	97
6		4	98	25	95
7		5	99	25	90
8		5	99	0	95
9		4.5	99	0	95

Reaction conditions: substrate (1 mmol), DCM (3 mL), m-CPBA (2 mmol) and catalyst (0.06 g) at room temperature

[a] Determined by GC with a CBP5 column (Shimadzu 30 m × 0.32 mm × 0.25 mm)

of the catalysts reveal that Fe₃O₄/SiO₂ catalyst with faster reaction rate, higher yield and selectivity shows better performance as compared to the earlier ones (Table 5, entry 13).

We also investigated the possibility of reusing of recovered catalysts for new reaction. Therefore, the catalyst was separated by external magnet, washed with EtOH, dried and reused directly for a subsequent round of reaction without further purification with no significant loss of activity, which validates its recyclability (Fig. 8). Moreover, the IR spectrum of Fe₃O₄/SiO₂ NPs after five reuses show that IR bands of the original skeletal vibration of Fe₃O₄/SiO₂ have no obvious change compared to fresh catalyst (Fig. 4c).

Table 5 Performance of different transition metal oxides for the epoxidation of styrene

Entry	Catalyst	Selectivity[a] (%)			Yield of SO[b] (%)/ref.
		SO[b]	BzA[c]	Others	
1	NiO nanodisks	60.2	7.6	35.6	38.6 [21]
2	Fe_3O_4	74.1	22.8	3.1	31.9 [22]
3	NiO	86.2	1.7	12.1	44.6 [2]
4	CoO	73.1	0.1	26.8	34.6 [2]
5	MoO_3	76.2	0.0	9.6	32.0 [2]
6	$Au-Yb_2O_3$	54.8	7.1	38.1	54.8 [23]
7	BaO/Ga_2O_3	58	0.0	42	58.0 [3]
8	Au/MgO	66.1	0.1	33.8	44.3 [24]
9	Au/CaO	60.2	6.3	19.2	32.3 [24]
10	Au/BaO	53.5	10.2	17.6	30.0 [24]
11	Au/SrO	44.8	11.7	26.0	23.7 [24]
12	$Au/meso-Al_2O_3$	69.0	23.0	8	84.3 [25]
13	Fe_3O_4/SiO_2	99	0.0	0.0	97 (This work)

[a] Selectivity (%)of product = (concentration of product/total concentration of all products) × 100

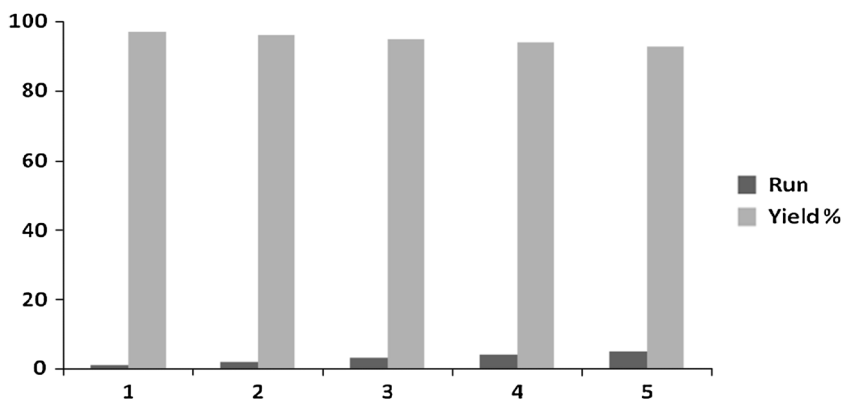[b] SO = styrene oxide

[c] BzA = benzaldehyde

Fig. 8 A comparison of the catalytic activity of fresh and reused catalyst for alkenes epoxidation. Reaction conditions: substrate (1 mmol), m-CPBA (2 mmol), DCM (3 mL), fresh or reused catalyst (0.06 g) 4 h at room temperature

Conclusions

In summary, we developed a facile, highly efficient, and eco-friendly procedure for the epoxidation of olefins in the presence of Fe_3O_4/SiO_2 as a heterogeneous catalyst at mild reaction conditions. The prepared catalyst is found to be efficient catalyst for the selective epoxidation of olefins to their corresponding products. This

heterogeneous catalyst is highly reactive in the epoxidation of a wide range of alkenes such as linear and cyclic ones. Moreover, easy preparation, handling and recovery, reusability and long-term stability of the catalyst, as well as excellent yields in shorter reaction time under mild reaction conditions, which are some advantages of this heterogeneous catalyst, make it a useful catalyst for further applications in the area of catalysis.

References

1. Cui HT, Zhang Y, Qiu ZG, Zhao LF, Zhu YL (2010) Synthesis and characterization of cobalt-substituted SBA-15 and its high activity in epoxidation of styrene with molecular oxygen. Applied Catal B 101:45–53
2. Choudhary VR, Jha R, Jana P (2008) Selective epoxidation of styrene to styrene oxide by TBHP using simple transition metal oxides (NiO, CoO or MoO3) as highly active environmentally-friendly catalyst. Catal Commun 10:205–207
3. Choudhary VR, Jha R, Jana P (2006) Epoxidation of styrene by TBHP to styrene oxide using barium oxide as a highly active/selective and reusable solid catalyst. Green Chem 8:689–690
4. Choudhary VR, Jha R, Chaudhari NK, Jana P (2007) Supported copper oxide as a highly active/selective catalyst for the epoxidation of styrene by TBHP to styrene oxide. Catal Commun 8:1556–1560
5. Khouw CB, Dartt CB, Labinger JA, Davis ME (1994) Studies on the catalytic oxidation of alkanes and alkenes by titanium silicates. J Catal 149:195–205
6. Xie J, Wang Y, Li Y, Wei Y (2011) Self-assembly preparation of Au/SiO2 catalyst and its catalysis for cyclohexane oxidation with air. React Kinet Mech Cat 102:143–154
7. He J, Zhai Q, Zhang Q, Deng W, Wang Y (2013) Active site and reaction mechanism for the epoxidation of propylene by oxygen over CuOx/SiO2 catalysts with and without Cs$^+$ modification. J Catal 299:53–66
8. Shi H-C, Wang X-Y, Hua R, Zhang Z-G, Tang J (2005) Epoxidation of α, β-unsaturated acids catalyzed by tungstate (VI) or molybdate (VI) in aqueous solvents: a specific direct oxygen transfer mechanism. Tetrahedron 61:1297–1307
9. Polshettiwar V, Varma RS (2010) Green chemistry by nano-catalysis. Green Chem 12:743–754
10. Shylesh S, Schunemann V, Thiel WR (2010) Magneticaly separable nanocatalysts: bridges between homogeneous and heterogeneous catalysis. Ange Chem Inter Edit 49:3428–3459
11. Lu AH, Salabas EL, Schuth F (2007) Magnetic nanoparticles: synthesis, protection, functionalization, and application. Ange Chem Inter Edit 46:1222–1244
12. Lu HC, Yi GS, Zhao SY (2004) Synthesis and characterization of multi-functional nanoparticles possessing magnetic, up-conversion fluorescence and bio-affinity properties. J Mater Chem 14:1336–1341
13. Grasset F, Dorson F, Molard Y (2008) One-pot synthesis and characterizations of bi-functional phosphor–magnetic @SiO2 nanoparticles: controlled and structured association of Mo6 cluster units and γ-Fe2O3 nanocrystals. Chem Commun 39:4729–4731
14. Gonzalez-Fernandez MA, Torres TE, Andr-Verg M, Costo R, de la Presa P, Serna CJ, Morales MP, Marquina C, Ibarra MR, Goya GF (2009) Magnetic nanoparticles for powerabsorption: optimizing size, shape and magnetic properties. J Solid State Chem 182:2779–2784
15. Polshettiwar V, Luque R, Fihri A, Zhu H, Bouhrara M, Basset J-M (2011) Magnetically recoverable nanocatalysts. Chem Rev 111:3036–3075
16. Lu ZY, Dai J, Song XN, Wang G, Yang WS (2008) Facile synthesis of Fe3O4/SiO2 composite nanoparticles from primary silica particles. Colloids Surf 317:450–456
17. Leng Y, Sato K, Shi Y, Li J-G, Ishigaki T, Yoshida T, Kamiya H (2009) Oxidation-resistant silica coating on gas-phase-reduced iron nanoparticles and influence on magnetic properties. J Phys Chem C 113:16681–16685

18. Morel A-L, Nikitenko SI, Gionnet K, Wattiaux A, Lai-Kee-Him J, Labrugere C, Chevalier B, Deleris G, Petibois C, Brisson A, Simonoff M (2008) Sonochemical Approach to the Synthesis of Fe3O4@SiO2 Core − Shell Nanoparticles with Tunable Properties. ACS Nano 2:847–856

19. Liu Y, Jia L (2008) Analysis of estrogens in water by magnetic octadecylsilane particles extraction and sweeping micellar electro kinetic chromatography. Microchem J 89:72–76

20. Wu C, He H, Gao H, Liu G, Ma R, An Y, Shi L (2010) Synthesis of Fe$_3$O$_4$@SiO$_2$@polymer nanoparticles for controlled drug release. Sci China Chem 53:514–518

21. Ren S, Yang C, Sun C, Hui Y, Dong Z, Wang J, Su X (2012) Novel NiO nanodisks and hollow nanodisks derived from Ni(OH)2 nanostructures and their catalytic performance in epoxidation of styrene. Materials Lett 80:23–25

22. Huang C, Zhang H, Sun Z, Zhao Y, Chen S, Tao R, Liu Z (2011) Porous Fe$_3$O$_4$ nanoparticles: synthesis and application in catalyzing epoxidation of styrene. J Colloid Interface Sci 364:298–303

23. Choudhary VR, Dumbre DK, Patil NS, Uphade BS, Bhargava SK (2013) Epoxidation of styrene by t-butyl hydroperoxide over gold nanoparticles supported on Yb$_2$O$_3$: effect of gold deposition method, gold loading, and calcination temperature of the catalyst on its surface properties and catalytic performance. J Catal 300:217–224

24. Patil NS, Uphade BS, Jana P, Bharagava SK, Choudhary VR (2004) Epoxidation of styrene by anhydrous t-butyl hydroperoxide over reusable gold supported on MgO and other alkaline earth oxides. J Catal 223:236–239

25. Yin D, Qin L, Liu J, Li C, Jin Y (2005) Gold nanoparticles deposited on mesoporous alumina for epoxidation of styrene: effects of the surface basicity of the supports. J Mole Catal A 240:40–48